JOURNAL OF CATALYSIS 66, 267–280 (1980)

Heterogeneous Catalysis in the Liquid-Phase Oxidation of Olefin

V. Oxidation of Cyclohexene with Supported Molybdenum–Chromium Binary Oxide Catalyst

KATSUOMI TAKEHIRA, TAKASHI HAYAKAWA, AND TOSHIO ISHIKAWA

Oxidation Laboratory, Catalysis Division, National Chemical Laboratory for Industry, Tsukuba Research Center, Yatabe, Ibaraki, 305, Japan

Received January 16, 1980; revised June 3, 1980

The oxidation of cyclohexene has been studied in the liquid phase, using as catalysts molybdenum–chromium binary oxides supported on γ-Al_2O_3. The activities were compared by measuring maximum rates of oxygen absorption. The binary system catalysts, in which the formations of chemical compounds were suggested, showed higher activities than the one component systems. The maximum rate was 0.4 order with respect to the catalyst in the region of low catalyst concentration; a much lower order was found for high concentration. There was a critical concentration of catalyst observed, above which the rate of oxidation dropped suddenly. For low catalyst concentration, the maximum rate proved to be first order with respect to the concentration of cyclohexene; a much higher order was observed for high concentrations. The apparent activation energies for oxidation ranged between 12.2 and 14.0 kcal/mol. Product distribution studies suggested that the epoxidation of cyclohexene with cyclohexenyl hydroperoxide proceeded on the molybdenum-rich catalysts and also that cyclohexenone was partly produced by the reaction between cyclohexenyl peroxy radicals and the catalyst. A degenerate chain branching mechanism is proposed in which the catalyst plays an important role in the initiation and termination steps.

I. INTRODUCTION

The liquid-phase oxidation of cyclohexene, catalyzed by soluble transition metal salts, has been studied extensively. The work reported so far on insoluble catalysts for the oxidation of cyclohexene is mainly that of Meyer *et al.* (*1*), Gould and Rado (*2*), and Neuburg *et al.* (*3–5*). They used one component metal oxides such as CoO, MnO_2, Cr_2O_3, etc., mainly in the form of insoluble catalysts. Recently the authors (*6–9*) studied this oxidation by using vanadium–chromium binary oxides as catalysts. The activity of the binary system was higher than the one component metal oxides, i.e., vanadium pentoxide and chromium(III) oxide separately, and depended on the catalyst structure which seemed to be largely influenced by its method of preparation. When the binary system was supported on SiO_2, the effect of interaction between SiO_2 and each metal oxide was more strongly observed than the effect of the binary system formation; the latter effect was preferably found on γ-Al_2O_3 carrier.

Molybdenum–chromium binary oxide supported on γ-Al_2O_3 (Mo–Cr–γ-Al_2O_3) also showed high activity (*8*) which may be attributable to the formation of chemical compounds as observed in the vanadium–chromium binary system (*7*). It was considered that the autoxidation of cyclohexene proceeds through the radical decomposition of 1-cyclohexenyl hydroperoxide (HPO), i.e., the degenerate chain branching mechanism, on the latter binary system (*7–9*). Also the termination reaction is reasonably expected on the heterogeneous metal oxide catalyst as has been reported by Neuburg *et al.* (*5*) and Srivastava *et al.* (*10–12*).

In the present work, Mo–Cr–γ-Al_2O_3 catalyst was prepared by a kneading method and its effect on kinetics of the

0021-9517/80/120267-14$02.00/0

liquid-phase oxidation of cyclohexene was studied. The effects of molybdenum: chromium composition, cyclohexene concentration, catalyst amount, oxygen partial pressure, and temperature on the reaction rate and the product distribution are discussed. The decomposition of *t*-butyl hydroperoxide (*t*-BuOOH) was also carried out for the purpose of studying the character of the binary system catalyst.

II. EXPERIMENTAL METHODS

1. Catalysts

The supported binary system catalysts were prepared by the kneading method as follows; a mixture of ammonium paramolybdate, chromium(III) nitrate, and alumina hydrate (Shokubai Kasei Co., Ltd.) as the raw materials was kneaded in the presence of small amount of water at 80°C for 5 hr, dried at 100°C for 1 day, and calcined at 450°C for 5 hr in air. The resulting catalyst was pulverized and used as 30–40 mesh particle size powder. The concentration of metal oxides (calculated as $MoO_3 + Cr_2O_3$) was 20 wt%. The symbol, composition of supported metal oxides (in terms of atom% of Cr/(Mo + Cr)), and specific surface area (S_s) are given in Table 1.

TABLE 1

Symbol, Composition of Supported Metal Oxides, and Specific Surface Area of Catalyst[a,b]

Symbol	Composition Cr/(Mo + Cr) (atom%)	Specific surface area: S_s (m²/g)
MoO_3–γ-Al_2O_3	0	288
Mo–Cr–γ-Al_2O_3-1	10	309
Mo–Cr–γ-Al_2O_3-2	20	301
Mo–Cr–γ-Al_2O_3-3	30	295
Mo–Cr–γ-Al_2O_3-5	50	290
Mo–Cr–γ-Al_2O_3-7	70	249
Cr_2O_3–γ-Al_2O_3	100	293

[a] Concentration of metal oxides (calculated as $MoO_3 + Cr_2O_3$) was 20 wt%.

[b] Specific surface area of γ-Al_2O_3 similarly prepared from the alumina hydrate was 220 m²/g.

2. Apparatus and Procedure

The oxidation was carried out using a 200 ml batch-system reactor with an oxygen recycling unit and a magnetic stirrer (*6*). Oxygen consumption was measured by a gas meter. It was verified that the kinetic results obtained were not influenced by the stirring speed. Cyclohexene (30.0 ml, purified by passing it over activated alumina to eliminate the hydroperoxide), benzene as solvent (40.0 ml), and *t*-BuOOH (0.1 ml) were used in each reaction, except when the effect of cyclohexene concentration was studied. *t*-BuOOH purified by distillation (40.0°C/25 mm Hg) was added such that reproducible results of oxidation were obtained (*8*).

The decomposition of *t*-BuOOH was performed in 10-ml reaction tubes attached to a wrist-action shaker to achieve vigorous agitation (*9*) using 25 mg of the binary catalyst and 5 ml of benzene solution of *t*-BuOOH (0.1 *M*) at 60°C under a nitrogen atmosphere.

3. Analyses of Reaction Products and Catalysts

The oxidation products 1-cyclohexenyl hydroperoxide (HPO), 2-cyclohexene-1-one (ONE), 2-cyclohexen-1-ol (OL), and cyclohexene oxide (OXIDE), and unconverted cyclohexene were determined by the iodometric method and gas chromatography (*6*).

t-BuOOH and its decomposition products *t*-butyl alcohol (*t*-BuOH), acetone, and di-*t*-butyl peroxide (*t*-Bu_2O_2) were identified, and then determined using the method reported previously (*9*).

The surface area of the catalyst was measured by the BET method using nitrogen, and its structure was studied by means of X-ray diffraction and infrared absorption (*6*). X-Ray photoelectron spectroscopy (XPS) measurements were carried out on a Du Pont ESCA 650 B using monochromatic AlK_α radiation (8).

III. RESULTS AND DISCUSSION

1. *Influence of the Molybdenum:Chromium Composition*

The results of the reactions for 4 hr with binary catalysts containing different molybdenum:chromium compositions are shown in Fig. 1, together with the results with one component systems, i.e., Mo–γ-Al_2O_3 and Cr–γ-Al_2O_3. Mo–γ-Al_2O_3 showed very low activity; its induction period of oxygen consumption (I.P.)[1] was very long (155 min) and its rate of oxygen consumption was extremely low. Cr–γ-Al_2O_3 was fairly active itself, and the activity increased further by the formation of Mo–Cr binary systems. The maximum rate of oxygen consumption per unit surface area of the catalyst (R_{max}/S), i.e., the specific activity, is shown in Fig. 2. The decomposition of *t*-BuOOH on the binary catalyst was a first-order reaction, and its products were *t*-BuOH, *t*-Bu_2O_2, and acetone, suggesting that *t*-BuOOH is decomposed homolitically as observed already with V–Cr–γ-Al_2O_3 (*9*). The specific activity of the binary system for the *t*-BuOOH decomposition was expressed by a first-order rate constant per unit surface area (k_1/S) (Fig. 2). The activity of R_{max}/S correlated well with that of k_1/S and also with the activity for initiation shown by I.P. in Fig. 1, suggesting that the autoxidation is initiated and accelerated by the radical decomposition of HPO on the binary catalyst.

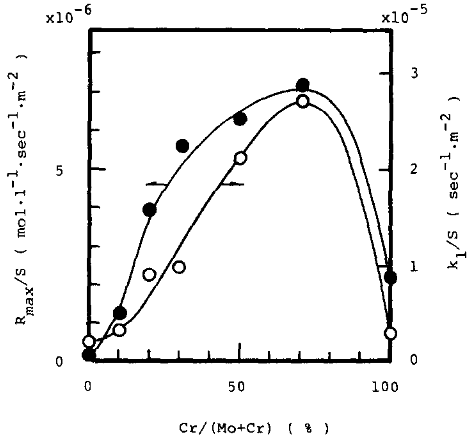

FIG. 2. Specific activity of Mo–Cr–γ-Al_2O_3 catalyst for the cyclohexene oxidation (R_{max}/S) and for the *t*-BuOOH decomposition (k_1/S).

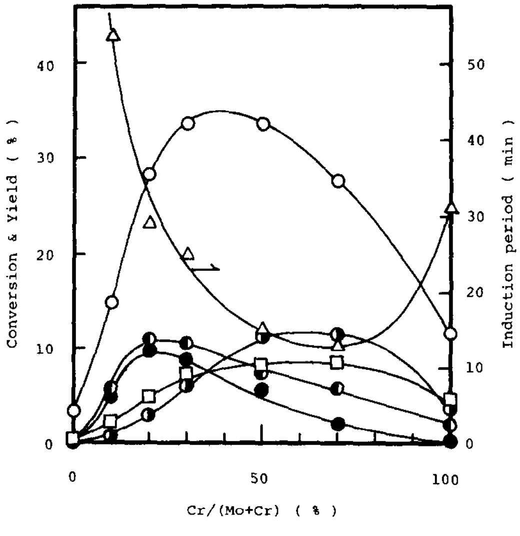

FIG. 1. Oxidation of cyclohexene with Mo–Cr–γ-Al_2O_3 catalysts. Cyclohexene, 30 ml; benzene, 40 ml; *t*-BuOOH, 0.1 ml; catalyst, 50 mg; reaction temperature, 60°C; reaction time, 4 hr; O_2 pressure, 1 atm; (△) induction period, (○) cyclohexene conversion. Yield, (◐) OL, (●) OXIDE, (□) HPO, (◑) ONE.

Concerning the product distribution, OXIDE and OL were produced maximally on the catalysts of high molybdenum content, HPO and ONE on the contrary on those of high chromium content (Fig. 1). It is thus considered that two types of active sites exist on the present binary catalyst; one composed mainly of molybdenum species catalyzes the epoxidation of cyclohexene with HPO and another of chromium species catalyzes the autoxidation as observed already in the vanadium–chromium binary catalyst (*6*–*8*).

The analytical results of surface state of Mo–Cr–γ-Al_2O_3 by XPS showed the valence state of molybdenum is about +6 because of the Mo3d5/2 values of 232.8–233.0 eV (*13*) on all the catalysts used. On

---

[1] I.P. was defined as a time at an intersecting point on a time axis of a maximum tangent line of oxygen consumption curve.

the other hand, the Cr2p3/2 binding energy of 577.6 eV on Mo–Cr–γ-Al$_2$O$_3$-1 shifted toward a slightly higher value of 578.0 eV on Mo–Cr–γ-Al$_2$O$_3$-7, and the value of spin-orbit splitting (*E*) of the Cr2p level decreased simultaneously from 9.8 eV on Mo–Cr–γ-Al$_2$O$_3$-1 to 9.5 eV on Mo–Cr–γ-Al$_2$O$_3$-7, when the chromium content in the binary system increased. These results suggest that the valence state of chromium is higher than +3 in the binary system of higher chromium content (*8*, *14*). The peak area ratios of Mo3d5/2 and Cr2p3/2 to Cls as a standard were plotted to the Mo:Cr composition (Fig. 3). Both the ratios are on the straight lines passing the origins, indicating that each of molybdenum and chromium distributes uniformly in proportion to the Mo:Cr composition.

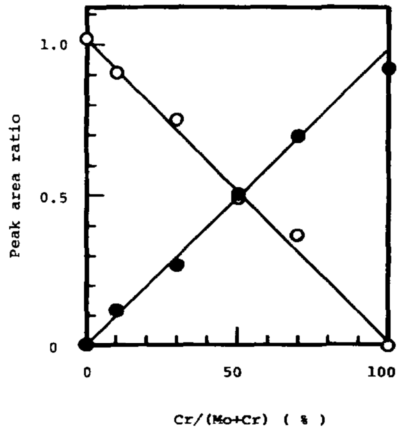

FIG. 3. Peak area ratios of Mo3d5/2 and Cr2p3/2 to Cls in XPS spectra; (○) (Mo3d5/2)/(Cls), (●) (Cr2p3/2)/(Cls).

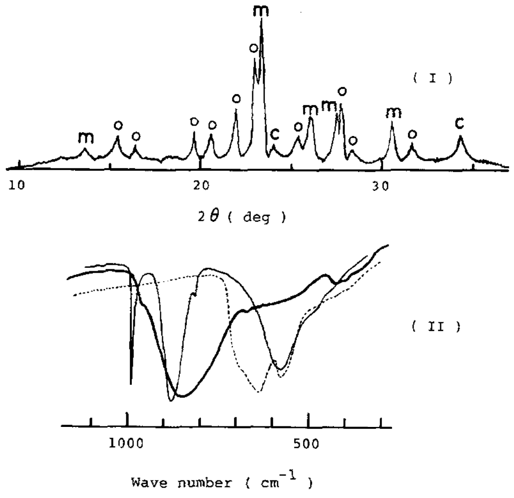

FIG. 4. X-Ray diffraction diagram (I) and ir absorption spectrum (II) of the Mo–Cr binary oxide, (I), (m) MoO$_3$, (c) Cr$_2$O$_3$: (II), (——) MoO$_3$, (-----) Cr$_2$O$_3$, (——) the binary oxide.

In the X-ray diffraction patterns or the ir absorption spectra of Mo–Co–γ-Al$_2$O$_3$ catalysts, only some broad peaks or absorption lines assigned to γ-Al$_2$O$_3$ were observed; the evidence of MoO$_3$, Cr$_2$O$_3$, or chromium molybdate supposed to be formed (*14*) was not obtained. An unsupported Mo–Cr (1:1) binary oxide was prepared from ammonium paramolybdate and chromium(III) nitrate by the same method as the catalyst preparation. Its X-ray diffraction pattern (I) and ir absorption spectrum (II) are shown in Fig. 4. The X-ray analysis showed several lines (o) which can be assigned neither to MoO$_3$ (m) nor to Cr$_2$O$_3$ (c); none of the reduced species of MoO$_3$ (e.g., Mo$_3$O$_7$, MoO$_2$, etc.) was detected. The ir spectrum differed clearly from those of MoO$_3$ and Cr$_2$O$_3$. A broad absorption band at 840–850 cm^{-1} is assigned to the [MoO$_4$] tetrahedron observed in the structure of some molybdates (*16*); the absorption band at about 990 cm^{-1} assigned to the octahedral [MoO$_6$] in MoO$_3$ was not observed clearly. After these, chromium molybdates containing the [MoO$_4$] tetrahedron may be formed in the binary system. Also when the binary system was supported on γ-Al$_2$O$_3$, such chemical compounds may be formed, resulting in the increase in catalytic activity. It is doubtful that molybdenum species catalyze the homolytic decomposition of HPO, though it can catalyze the epoxidation with HPO (*8*). Therefore, the activity for the radical decomposition may be due to chromium species; this increased activity observed in the binary system may be based upon a change in the coordination state around the chromium. This latter may be changed by the chemical compound formation of the chromium.

2. *Kinetics of the Reaction*

In order to clarify the oxidation mechanism of the binary system, the kinetics of oxidation was studied using the most active catalyst: Mo–Cr–γ-Al_2O_3-7. Mo–Cr–γ-Al_2O_3-2, on which the epoxidation was observed together with the autoxidation, was also used as a catalyst for comparison.

The oxygen consumption curves when changing the amount of Mo–Cr–γ-Al_2O_3-7 are shown in Fig. 5. The R_{max} increased and the I.P. was shortened when increasing the catalyst amount up to about 50 mg, above which the R_{max} increments became very small; the I.P. was also lengthened with larger amounts of catalyst. When the amount of 700 mg was reached, oxygen consumption was not observed for an 8 hr reaction except that a small amount of oxygen was absorbed at the beginning of the reaction. The values of R_{max} and the rate of oxygen consumption at the beginning of reaction (R_b) with Mo–Cr–γ-Al_2O_3-7 catalyst are shown in Fig. 6; the reciprocal of I.P. is shown in Fig. 7. Also when using Mo–Cr–γ-Al_2O_3-2, a similar result was observed; oxygen consumption was not observed in the presence of 2000 mg of the catalyst even when an 8 hr reaction was carried out. The results are shown in Figs. 6

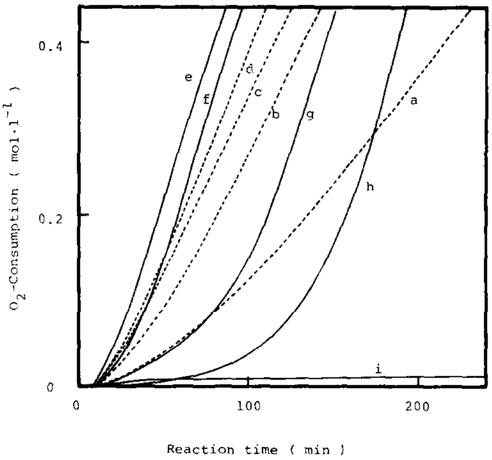

FIG. 5. Oxygen consumption curves when using various amounts of Mo–Cr–γ-Al_2O_3-7 catalyst. Cyclohexene, 30 ml; benzene, 40 ml; *t*-BuOOH, 0.1 ml; reaction temperature, 60°C; oxygen pressure, 1 atm; amount of the catalyst, (a) 1.8, (b) 5.2, (c) 10, (d) 20, (e) 75, (f) 200, (g) 400, (h) 500, (i) 700 mg.

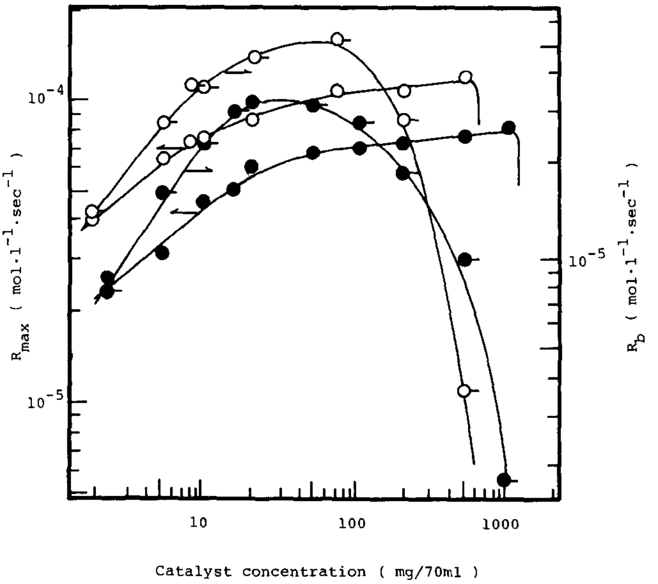

FIG. 6. Rates of oxygen consumption: R_{max} and R_b. (○,○-) Mo–Cr–γ-Al_2O_3-7; (●,●-) Mo–Cr–γ-Al_2O_3-2.

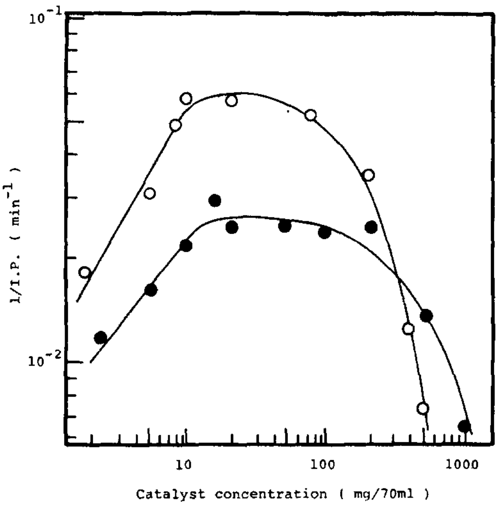

FIG. 7. Reciprocal of induction period. (○) Mo–Cr–γ-Al_2O_3-7; (●) Mo–Cr–γ-Al_2O_3-2.

and 7. The order of the R_{max} with respect to the catalyst concentration was 0.40 and 0.43 for Mo–Cr–γ-Al_2O_3-7 and -2, respectively, at low concentrations; both the values were nearly equal to zero at the high concentrations.

When the autoxidation of cyclohexene proceeds under sufficiently long oxidation chains as follows (R, cyclohexenyl radical; M, catalyst):

$$\mathrm{ROOH} \xrightarrow{\mathrm{M}} \mathrm{RO}\cdot \text{ and } \mathrm{RO_2}\cdot \xrightarrow{\mathrm{RH}} \mathrm{R}\cdot, \quad (1)$$

$$\mathrm{R}\cdot + \mathrm{O_2} \rightarrow \mathrm{RO_2}\cdot, \quad (2)$$

$$\mathrm{RO_2}\cdot + \mathrm{RH} \xrightarrow{k_p} \mathrm{ROOH} + \mathrm{R}\cdot, \quad (3)$$

$$\mathrm{RO_2}\cdot + \mathrm{RO_2}\cdot \xrightarrow{k_t} \text{nonradicals} + \mathrm{O_2}. \quad (4)$$

If oxygen evolved from the biradical termination (4) is neglected with respect to oxygen absorbed in the propagation, the rate of oxidation can be expressed as:

$$-d[\mathrm{O_2}]/dt = (R_i/2k_t)^{1/2}k_p[\mathrm{RH}] \quad (5)$$

where R_i stands for the rate of free radical initiation. At the low catalyst concentration, Eq. (7) is obtained:

$$R_i = k_i[\mathrm{ROOH}][\mathrm{M}], \quad (6)$$

$$-d[\mathrm{O_2}]/dt = (k_i/2k_t)^{1/2}k_p[\mathrm{RH}][\mathrm{ROOH}]^{1/2}[\mathrm{M}]^{1/2}. \quad (7)$$

It is considered that HPO is decomposed via an adsorption equilibrium of HPO on the binary catalyst (*4*, *17*). Under the condition that the concentration of HPO is far higher than that of the catalyst, Eq. (7) becomes:

$$-d[\mathrm{O_2}]/dt = (k_i'/2k_t)^{1/2}k_p[\mathrm{RH}][\mathrm{M}]^{1/2}. \quad (8)$$

At high catalyst concentrations, the rates of formation and decomposition of HPO become equal; a steady-state concentration of HPO is attained complying with the equation:

$$[\mathrm{ROOH}]_\infty = \frac{k_p{}^2[\mathrm{RH}]^2}{2k_ik_t[\mathrm{M}]}. \quad (9)$$

From this the limiting theoretical rate of oxidation becomes:

$$-d[\mathrm{O_2}]/dt = k_p{}^2[\mathrm{RH}]^2/k_t. \quad (10)$$

The results shown in Fig. 6 can be qualitatively explained by Eqs. (8) and (10), which relate the reaction order with respect to catalyst. The values found as the limiting rate in Fig. 6 were 1/20–1/30 of the theoretical value: 2.6×10^{-3} mol/liter · sec, given by Eq. (10) when using values of $k_p{}^2/2k_t$ obtained by Mayo *et al.* (*18*). The present values are far smaller than 3.3×10^{-4}–7.5×10^{-4} and 7.0×10^{-4} mol/liter · sec obtained when using MnO_2 catalyst (*5*) and cobaltous acetate catalyst (*19*), respectively. Moreover, in a reaction for reference, $Co(acac)_2$ (10^{-2} mol/liter) showed a rate of 5.6×10^{-4} mol/liter · sec under conditions similar to the reaction with Mo–Cr–γ-Al_2O_3 catalyst. This value suggests that the reaction is not diffusion limited. These results indicate that Mo–Cr–γ-Al_2O_3 catalyst has large inhibiting properties. The R_b and the reciprocal of I.P. showed a similar tendency with respect to the catalyst concentration, indicating that the radical chain reaction is initiated by the decomposition of HPO on the catalyst. The reaction orders of R_b with respect to the catalysts of low concentration were larger than the value of 1 (Fig. 6). It has been established (*20*) that for short chain length a more general expression for the rate of oxygen consumption can be derived:

$$-d[O_2]/dt = 3R_i/2 + (R_i/2k_t)^{1/2}k_p[RH]. \qquad (11)$$

If the rate of free radical initiation is proportional to the concentration of catalyst (Eq. (6)), the increase of the reaction order with respect to catalyst from the value 0.5 will depend on the influence on the term $3R_i/2$. A lowering of the R_b and an increase of the I.P. observed when using a large amount of catalyst (Figs. 6 and 7) may be due to inhibition by the catalyst or to the adsorption of HPO on inactive sites of the catalyst.

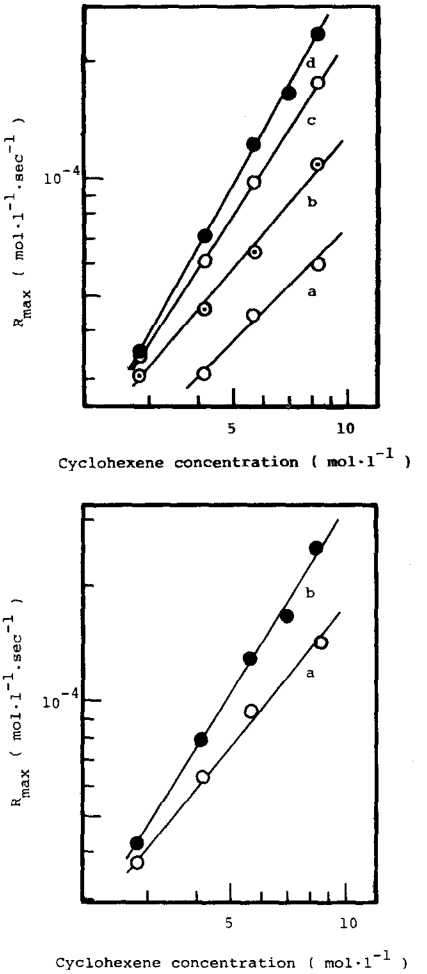

FIG. 8. (a) Rate dependence with respect to cyclohexene concentration. Catalyst, Mo–Cr–γ-Al_2O_3-2, (a) 5, (b) 10, (c) 20, (d) 50 mg; reaction temperature, 60°C. (b) Rate dependence with respect to cyclohexene concentration. Catalyst, Mo–Cr–γ-Al_2O_3-7, (a) 5, (b) 10 mg; reaction temperature, 60°C.

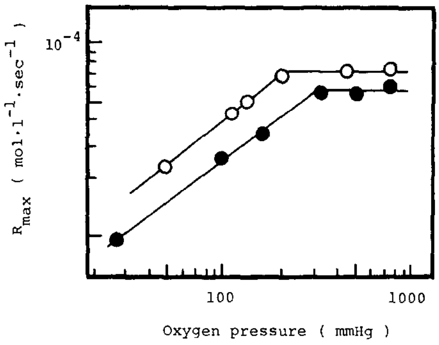

FIG. 9. Rate dependence with respect to oxygen pressure. Catalyst, (●) Mo–Cr–γ-Al_2O_3-2, 20 mg; (○) Mo–Cr–γ-Al_2O_3-7, 10 mg; reaction temperature, 60°C.

The dependence of the rate of oxidation on the concentration of cyclohexene is shown in Fig. 8, with changing amounts of catalyst. The value of the reaction order with respect to the cyclohexene concentration varied depending on the amount of catalyst used; the value was 1.8, 1.5, 1.2, and 1.0 when using 50, 20, 10, and 5 mg, respectively, of Mo–Cr–γ-Al_2O_3-2 (Fig. 8a), and 1.6 and 1.2 when using 10 and 5 mg, respectively, of Mo–Cr–γ-Al_2O_3-7 (Fig. 8b). These values can be explained by Eqs. (8) and (10). When a large amount of the catalyst was used, the value neared to 2 as shown by Eq. (10); on the contrary, the value decreased to 1, by Eq. (8), as the amount of catalyst was reduced.

The influence of the oxygen pressure is shown in Fig. 9. At low O_2 pressure, the order of the reaction, with respect to oxygen, was between 0.7 and 0.8; the order was zero complying with Eq. (8) or (10) at atmospheric pressure.

The influence of the reaction temperature is shown in Fig. 10. An apparent activation energy (E_{ob}), obtained from the R_{max}, changed somewhat depending on the

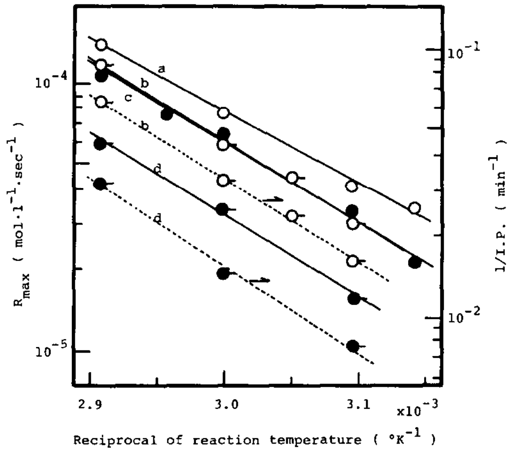

FIG. 10. Influence of reaction temperature on reaction rate (——) and induction period (-----). Catalyst, Mo–Cr–γ-Al_2O_3-7, (a) 10, (b) 5 mg; Mo–Cr–γ-Al_2O_3-2, (c) 20, (d) 5 mg.

amount of catalyst used; the value of E_{ob} was 12.2 and 13.9 kcal/mol with 10 and 5 mg, respectively, of Mo–Cr–γ-Al_2O_3-7. It was 13.5 and 14.0 kcal/mol with 20 and 5 mg, respectively, of Mo–Cr–γ-Al_2O_3-2. According to Eqs. (8) and (10), E_{ob} can be expressed by either Eq. (12) or Eq. (13):

$$E_{ob} = E_p + (E_i - E_t)/2, \qquad (12)$$

$$E_{ob} = 2E_p - E_t \qquad (13)$$

where E_p = activation energy of the propagation step, E_i = activation energy of the initiation, and E_t = activation energy of the biradical termination of peroxy radicals. Equation (12) can be adopted at low catalyst concentrations, and, accordingly, the value of E_{ob} may be calculated as about 14 kcal/mol. For the oxidation of cyclohexene, the following values were obtained: E_p = 8.5 kcal/mol by Bateman and Gee (*21*), and E_p = 7.5 kcal/mol and E_t = 4.5 kcal/mol by Howard and Cobb (*22*). The adoption of the values reported by Howard and Cobb and 14 kcal/mol as E_{ob} into Eq. (12) gave the value of E_i = 17.5 kcal/mol. Values from the literature of E_{ob} = 11.4–13.0 kcal/mol were reported for the oxidation of cyclohexene with MnO_2 catalyst (*5*). Arrhenius plots of the reciprocal of I.P., a part of which are shown in Fig. 10, gave the following values of apparent activation energy: 13.0 and 14.2 kcal/mol with 10 and 5 mg, respectively, of Mo–Cr–γ-Al_2O_3-7, and 12.9 and 14.9 kcal/mol with 20 and 5 mg, respectively, of Mo–Cr–γ-Al_2O_3-2.

3. Reaction Products

The oxidation products recognized in the present work were HPO, ONE, OL, and OXIDE. The molar percentage of each product is shown in Figs. 11 and 12, as catalyst concentration and the reaction temperature are varied. All the reactions were carried out until the amount of oxygen absorbed reached about 1500 ml NTP, except when the reaction was stopped at 4 hr because the catalyst concentration was too small to give a sufficient rate of oxidation (Fig. 11).

On Mo–Cr–γ-Al_2O_3-7 catalyst (Fig. 11a), the selectivity of OXIDE showed a low value of about 5%; OXIDE may be formed mainly via the addition of peroxy radical to cyclohexene (*18, 23*):

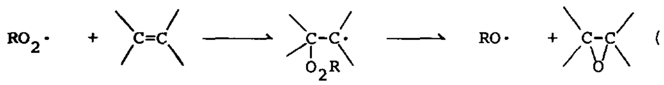

(14)

When increasing the amount of catalyst, a decrease of HPO and an increase of ONE were observed; the amounts of OL and OXIDE did not significantly change. On Mo–Cr–γ-Al_2O_3-2 catalyst (Fig. 11b), a fairly large amount of OXIDE and OL was observed; conversely those of HPO and ONE were small. The results support the hypothesis that the epoxidation of cyclohexene with HPO is catalyzed by molybde-

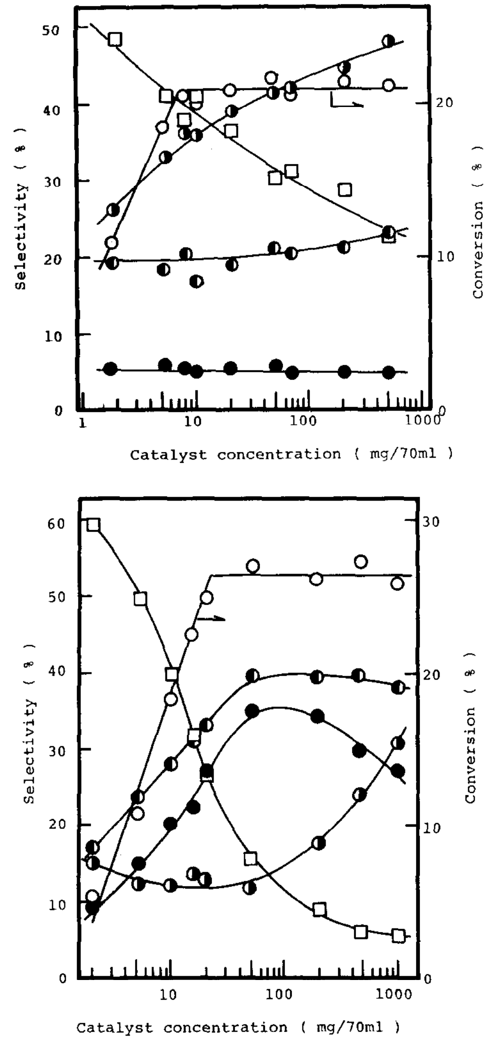

FIG. 11 (a) Influence of catalyst concentration on product distribution. Catalyst, Mo–Cr–γ-Al_2O_3-7; (○) cyclohexene conversion; products, (□) HPO, (◑) ONE, (◐) OL, (●) OXIDE. (b) Influence of catalyst concentration on product distribution. Catalyst, Mo–Cr–γ-Al_2O_3-2; (○) cyclohexene conversion; products, (□) HPO, (◑) ONE, (◐) OL, (●) OXIDE.

num species on Mo–Cr–γ-Al_2O_3-2. The product distribution obtained at low conversion, when using a small amount catalyst (Fig. 11), shows that the first oxidation product is HPO which is then converted into ONE and OL or epoxidizes cyclohexen. Though the amount of oxygen consumed was fixed at a constant value of 1500 ml NTP in the reactions with both the catalysts, a difference in the value of cyclohexene conversion was observed. Conversion was 21% on Mo–Cr–γ-Al_2O_3-7 and 27% on Mo–Cr–γ-Al_2O_3-2; the difference of 6% suggests that cyclohexene is consumed by the successive epoxidation on the latter catalyst.

When further increasing the amount of catalyst, the concentration of catalyst reached a limiting value where the oxidation was inhibited almost completely (Fig. 6). Above the limiting concentration of catalyst, only ONE was detected with a selectivity above 90%. The result suggests that ONE forms selevtively by the inhibition reaction. Two possible types of reactions catalyzed by chromium species are considered. First is a nonradical decomposition of hydroperoxide as has been reported in the oxidation of ethylbenzene (*24*):

$$\text{ROOH} \xrightarrow{Cr^{n+}} \text{ONE} + H_2O. \qquad (15)$$

The second is the reaction between peroxy radicals and the catalyst which was proposed by Ravens (*25*) and further observed with the ions of Mn^{2+} (*26*) and Co^{2+} (*27*):

$$RO_2\cdot + Cr^{n+} \rightarrow \text{ONE} + Cr^{(n+1)} + OH^-\cdot \qquad (16)$$

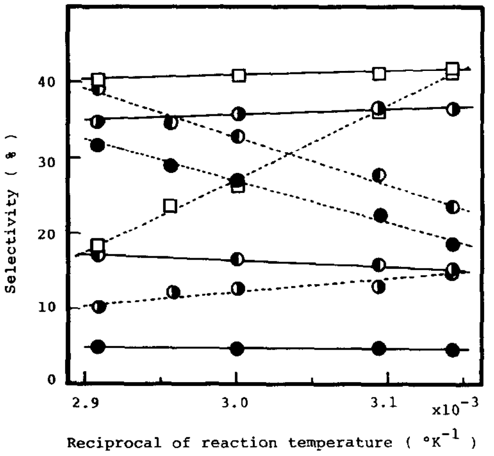

FIG. 12. Influence of reaction temperature on product distribution. Catalyst, (——) Mo–Cr–γ-Al_2O_3-7, 10 mg; (-----) Mo–Cr–γ-Al_2O_3-2, 20 mg; products, (□) HPO, (◑) ONE, (◐) OL, (●) OXIDE.

The influence of the reaction temperature is shown in Fig. 12. When the reaction temperature varied, the selectivity of each product did not change particularly on Mo–Cr–γ-Al_2O_3-7. However, on Mo–Cr–γ-Al_2O_3-2, the increments of OL and OXIDE, at the expense of HPO, was observed as the reaction temperature was raised. Epoxidation was favored at the high temperature. An activation energy of the epoxidation of 2-methyl-2-pentene with cumyl hydroperoxide, calculated from the data obtained by Sheng and Zajacek (*28*), using molybdate as catlayst, was 22.3 kcal/mol. This is higher than the value of E_{0b} obtained in the present work, supporting the result that epoxidation was favored at high temperatures.

4. *Inhibition on the Catalyst*

As mentioned above, Mo–Cr–γ-Al_2O_3 catalyst works as a promoter by decomposing, homolytically, HPO. On the other hand, it also works as an inhibitor of autoxidation. In order to clarify the mechanism of inhibition, the following studies were carried out.

TABLE 2

Product Distribution before (95 min) and after (140 min) the Addition of Large Amount of Catalyst

Catalyst	Reaction time (min)	Selectivity (%)			
		HPO	ONE	OL	OXIDE
Mo–Cr–γ-Al_2O_3-2	95	41.9	14.7	22.9	20.5
	140	5.2	49.1	23.9	21.8
Mo–Cr–γ-Al_2O_3-7	95	34.6	30.5	29.9	5.0
	140	3.4	68.2	24.6	3.8

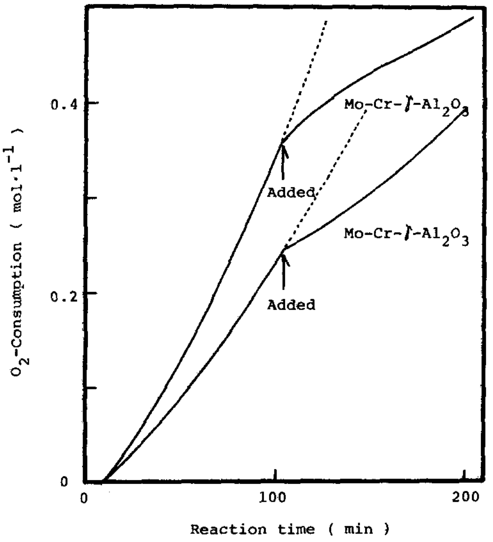

FIG. 13. Oxygen consumption as a function of time when adding a large amount of catalyst in the course of reaction. Catalyst amount up to 104 min, Mo–Cr–γ-Al_2O_3-7: 10 mg, Mo–Cr–γ-Al_2O_3-2: 20 mg; the final amount, Mo–Cr–γ-Al_2O_3-7: 2010 mg, Mo–Cr–γ-Al_2O_3-2: 5020 mg; cyclohexene, 30 ml; benzene, 40 ml; *t*-BuOOH, 0.1 ml; reaction temperature, 60°C; oxygen pressure, 1 atm.

A cyclohexene oxidation was studied with Mo–Cr–γ-Al_2O_3-7 catalyst concentration of 10 mg/ml, and the reaction continued for about 100 min. A large amount of the catalysts, 2000 mg, which had completely inhibited the oxidation (Fig. 6), was added into the reaction, and the oxidation was allowed to proceed. The change of the oxygen consumption curve is shown in Fig. 13. A similar experiment was performed also with Mo–Cr–γ-Al_2O_3-2, being started with 20 mg of catlayst and then adding 5000 mg (Fig. 13). In both the cases, the oxygen consumption was inhibited but not stopped by the addition of large amounts of catalyst. This may be due to the existence of relatively large amount of HPO. That is, as reported by Mukherjee and Graydon (*29*) and Fukuzumi *et al.* (*30*), there may exist a limiting ratio of HPO to the catalyst, below which no oxidation proceeds. The product distributions before and after the addition of large amount of catalyst, i.e., at the reaction time of 95 and 140 min, respectively, are shown in Table 2. A large increase of ONE at the expense of HPO was observed on both the catalysts.

Some oxidation experiments were carried out using a large amount of the catalysts in the presence of 2,2′-azo-bis-isobutyronitrile (AIBN) as a radical initiator (Fig. 14). Even in the presence of AIBN, the oxidation was retarded when using 2000

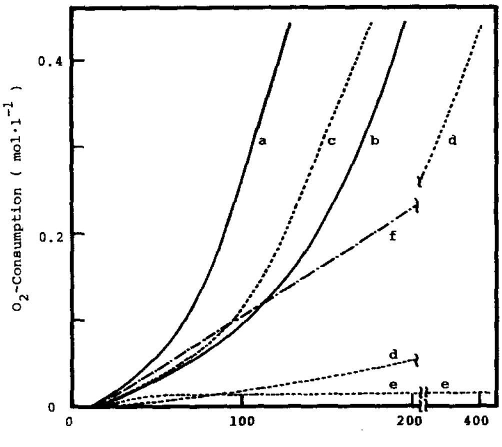

FIG. 14. Inhibition of the oxidation in the presence of AIBN when using a large amount of Mo–Cr–γ-Al_2O_3-7 (——) or Mo–Cr–γ-Al_2O_3-2 (-----). Cyclohexene, 30 ml; benzene, 40 ml; concentration of AIBN, 0.05 mol/liter; reaction temperature, 60°C; oxygen pressure, 1 atm; amount of catalyst, (a) 700, (b) 2000, (c) 2000, (d) 5000, (e) 10,000 mg, (f) without catalyst.

or 5000 mg of Mo–Cr–γ-Al_2O_3-2, or 2000 mg of Mo–Cr–γ-Al_2O_3-7; use of 10,000 mg of Mo–Cr–γ-Al_2O_3-2 inhibited the oxidation for 400 min or more. Such an inhibition observed even when radical initiators are present suggests that radicals are inactivated by the catalyst, that is, a main termination on the catalyst is not the nonradical decomposition of HPO, i.e., reaction (15), but reaction (16). The oxidation results are shown in Table 3. The values of R_{max} were similar to those obtained when no AIBN was added; the increase of ONE observed at the expense of HPO when the amount of catalyst increased was also similar to the result shown in Fig. 11. When 10,000 mg of Mo–Cr–γ-Al_2O_3-2 was added, only ONE was detected with a selectivity above 90%, also supporting reaction (16) as the main termination.

After a cyclohexene oxidation for 60 min using 300 mg of Mo–Cr–γ-Al_2O_3–7 or 200 mg of Mo–Cr–γ-Al_2O_3-2, stirring was interrupted in order to allow the catalyst particles to settle. Just before the interruption, the rate of oxygen consumption was 1.12×10^{-4} or 7.4×10^{-5} mol/liter · sec for Mo–Cr–γ-Al_2O_3-7 or Mo–Cr–γ-Al_2O_3-2, respectively. Each sample of the supernatant reaction liquid, when replaced in a fresh reactor without catalyst, showed a sharp decrease in the rate of oxidation to values of about 5×10^{-6} mol/liter · sec corresponding to the uncatalyzed reaction. This indicates that there was no homogeneous catalysis resulting from dissolved catalyst species in either oxidation.

An autoxidation of α-methylstyrene, an easily polymerizable olefin, proceeds almost completely by the addition mechanism (*23*), and accordingly can be initiated by a catalyst which activates oxygen molecules. This can be observed using Co(II) acetylacetonate (*31*). Two solutions, each of which contained 30 ml of α-methylstyrene and 40 ml of benzene, were prepared and oxidized at 60°C for 5 hr using 50 mg of Mo–Cr–γ-Al_2O_3-7 or Mo–Cr–γ-Al_2O_3-2, respectively. Neither of the two showed the

TABLE 3

Product Distribution and Rate of Oxidation in the Presence of AIBN[a]

Catalyst	Amount of catalyst (mg)	Selectivity (%)				R_{max} (mol/liter · sec) ($\times 10^{-5}$)
		HPO	ONE	OL	OXIDE	
Mo–Cr–γ-Al_2O_3-7	700	24.7	48.4	23.2	3.7	10.5
	2000	14.8	57.8	23.0	4.4	10.4
Mo–Cr–γ-Al_2O_3-2	2000	18.8	30.7	29.5	21.0	8.2
	5000	15.7	34.8	30.5	19.0	8.4

[a] Concentration of AIBN, 0.05 mol/liter; cyclohexene, 30 ml; benzene, 40 ml; reaction temperature, 60°C; amount of oxygen consumed, 1500 ml NTP.

oxygen absorption, suggesting that the ability for oxygen activation of these catalysts is very small.

5. *Reaction Mechanism*

The kinetics already described have been derived on the assumption that the catalyst works only as an initiator. However, the experimental results cannot be explained by such a simple mechanism, and indicate that the termination reaction (16) has an important role in the oxidation. As already reported, using V–Cr–γ–Al_2O_3 catalyst, the rate of initiation increased by the addition of *t*-BuOOH until the ratio of *t*-BuOOH to the catalyst amount reached a limiting value, beyond which no marked increase in the initiation rate was observed (*8*). Such a phenomenon can be reasonably expected also in the present study using Mo–Cr–γ–Al_2O_3 catalyst. This indicates that radical generation proceeds through the decomposition of hydroperoxide adsorbed on the heterogeneous catalyst surface (*4, 29*). This can be well understood when considering that an equilibrium of complex formation was observed between hydroperoxide and catalyst in the homogeneous oxidation (*32*). The adsorbed hydroperoxide may be decomposed homolytically via one electron transfer between itself and chromium ion on the catalyst.

The simplest reaction mechanism which accounts for many of the observed phenomena is presented. The initiation proceeds via the adsorption equilibria:

$$\mathrm{ROOH} + \mathrm{Cr}^{n+} \overset{K_1}{\rightleftharpoons} (\mathrm{ROOH} \cdots \mathrm{Cr}^{n+}), \quad (17)$$

$$(\mathrm{ROOH} \cdots \mathrm{Cr}^{n+}) \xrightarrow{k_2} \mathrm{RO}\cdot + \mathrm{Cr}^{(n+1)+} \cdots \mathrm{OH}^-, \quad (18)$$

$$\mathrm{ROOH} + \mathrm{Cr}^{(n+1)+} \cdots \mathrm{OH}^- \xrightarrow{k_3} \mathrm{RO_2}\cdot + \mathrm{H_2O} + \mathrm{Cr}^{n+}, \quad (19)$$

$$\mathrm{RO}\cdot + \mathrm{RH} \xrightarrow{k_4} \mathrm{ROH} + \mathrm{R}\cdot. \quad (20)$$

This is followed by the propagation step:

$$\mathrm{R}\cdot + \mathrm{O_2} \xrightarrow{k_0} \mathrm{RO_2}\cdot, \quad (2)$$

$$\mathrm{RO_2}\cdot + \mathrm{RH} \xrightarrow{k_p} \mathrm{RO_2H} + \mathrm{R}\cdot. \quad (3)$$

As the termination step, reaction (16), which produces ONE, may be added to the biradical termination (4) producing both of ONE and OL:

$$\mathrm{RO_2}\cdot + \mathrm{RO_2}\cdot \xrightarrow{k_t} \mathrm{ONE} + \mathrm{OL} + \mathrm{O_2}, \quad (4)$$

$$\mathrm{RO_2}\cdot + \mathrm{Cr}^{n+} \xrightarrow{k_t'} \mathrm{ONE} + \mathrm{Cr}^{(n+1)+} \cdots \mathrm{OH}^-. \quad (16)$$

Neuburg *et al.* (*5*) proposed a mechanism composed of the following biradical termination instead of reaction (16) for the oxidation of cyclohexene on MnO_2 catalyst. In this reaction nearly equal amounts of ONE and OL were produced:

$$\mathrm{RO_2}\cdot + \mathrm{Cr}^{n+} \xrightarrow{Kt} (\mathrm{RO_2} \cdots \mathrm{Cr}^{n+}), \quad (21)$$

$$\mathrm{RO_2}\cdot + (\mathrm{RO_2} \cdots \mathrm{Cr}^{n+}) \xrightarrow{k_t''} \text{inactive products}. \quad (22)$$

This mechanism was also adopted to the oxidations of cumene on NiO catalyst (*10*), cyclohexene, etc. on MnO_2 catalyst (*11*), and tetralin on NiO–Al_2O_3 catalyst (*12*), because ONE and OL were produced in nearly equal amounts. Already in the homogeneous oxidation of tetralin, a possibility of a similar mechanism was suggested by Kamiya and Ingold (*33*). He also, however, considered a termination reaction (16). Reaction (16) was recognized to be prominent in the reaction between *t*-alkyl peroxy radicals and Mn(II) ions (*34*). *sec*-Alkyl peroxy radicals may produce ketones selectively by this reaction, as reported by Mizukami and Imamura (*35*) in the oxidation of tetralin by chromium catalyst. Also in the present work, the remarkable increase in the ONE selectivity observed using a large amount of the catalyst supports reaction (16) as the termination.

Using the steady-state approximation for the mechanism mentioned above, the rate of free radical initiation (R_i) will be given by:

$$R_i = 2k_t[RO_2 \cdot]^2 + k_t'[RO_2 \cdot][Cr^{n+}]. \quad (23)$$

For sufficiently long reaction chains, the rate of oxidation can be derived:

$$-d[O_2]/dt = k_p[RO_2 \cdot][RH] = \frac{2k_pR_i[RH]}{k_t'[Cr^{n+}] + (k_t'^2[Cr^{n+}]^2 + 8R_ik_t)^{1/2}}. \quad (24)$$

If the termination reaction of peroxy radical on the catalyst surface, indicated by reaction (16), is negligible compared to the biradical termination (4), Eq. (5) is obtained.

When the limiting rate of oxidation is reached, it is assumed that the rate of formation of hydroperoxide through reaction (3) becomes equal to its rate of decomposition on the catalyst surface, R_d. In these circumstances the total rate of hydroperoxide formation will be:

$$\frac{d[ROOH]}{dt} = \frac{2k_pR_i[RH]}{k_t'[Cr^{n+}] + (k_t'^2[Cr^{n+}]^2 + 8R_ik_t)^{1/2}} - R_d \equiv 0. \quad (25)$$

HPO may be decomposed into radicals through reactions (17)–(19); a part of peroxy radicals formed through reaction (19) can be changed into ONE through reaction (16), resulting in no participation in the chain reaction. Though reaction (15) cannot be completely overlooked, it may be more reasonable to consider a combination of reaction (16) and (19) in order to explain the formation of ONE from HPO (Table 2), as reported by Mizukami and Imamura (*35*). This combination is also supported by the fact that water drops formed on the reactor wall, though its amount was not quantitated, when using a large amount of the catalyst.

It is assumed that R_i and R_d are linearly related as:

$$R_i = \alpha R_d \quad (26)$$

where α is the fraction of hydroperoxide decomposed contributing to radical initiation. Then the limiting rate of oxidation will be given as:

$$-d[O_2]/dt = k_p[RH](\alpha k_p[RH] - k_t'[Cr^{n+}])/2k_t. \quad (27)$$

Thus, Eqs. (24) and (27) were obtained instead of Eqs. (5) and (10), respectively, by introducing reaction (16) and the constant α. For a small enough value of $k_t'[Cr^{n+}]$, the reaction order with respect to the catalyst will become to 0.5, because R_i may be proportional to the catalyst concentration $[Cr^{n+}]$. When the rate of termination (16) of peroxy radical on the catalyst surface becomes competitive with the biradical termination (4), the reaction order will be less than 0.5. The values of 0.40 and 0.43 observed with Mo–Cr–γ-Al_2O_3-7 and -2, respectively, at low catalyst concentration suggests that the termination (16) cannot be ignored. As the catalyst concentration increased, the reaction order with respect to the catalyst became far lower (Fig. 6), indicating an increase of this contribution. In these circumstances, the reaction order with respect to cyclohexene was found between 1.0 and 2.0 (Fig. 8). Such an apparent order possibly results from a transition between these more normal responses to Eqs. (24) and (27). When the concentration of catalyst further increased, the limiting rate of oxidation was reached (Eq. (27)); its value was far smaller than the value obtained from Eq. (10), as mentioned already. It can be seen from Eq. (27) that for high catalyst concentration a point must be reached where $k_t'[M^{n+}] = k_p[RH]$ and inhibition will become complete.

From the present results, we conclude as follows: Mo–Cr–γ-Al_2O_3 catalyst accelerates the autoxidation of cyclohexene by decomposing homolytically HPO and simultaneously inhibits it by reacting with the peroxy radical (Eq. (16)). HPO is converted into ONE through a combination of reactions (19) and (16). These reactions which proceed via one electron transfer may be catalyzed by chromium species on the catalyst. Simultaneously, the epoxidation of cyclohexene with HPO may occur on its molybdenum species. The increase of activity observed on the Mo–Cr binary catalyst (Fig. 1) may be due to the changes of the coordination states around chromium atom.

REFERENCES

1. Meyer, C., Clément, G., and Balaçeanu, J.-C., *Proc. 3rd Int. Congr. Catal. 1964* **1**, 184 (1965).
2. Gould, E. S., and Rado, M., *J. Catal.* **13**, 238 (1969).
3. Neuburg, H. J., Basset, J. M., and Graydon, W. F., *J. Catal.* **25**, 425 (1972).
4. Neuburg, H. J., Phillips, M. J., and Graydon, W. F., *J. Catal.* **33**, 355 (1974).
5. Neuburg, H. J., Phillips, M. J., and Graydon, W. F., *J. Catal.* **38**, 33 (1976).
6. Takehira, K., and Ishikawa, T., *Bull. Chem. Soc. Japan* **49**, 2351 (1976).
7. Takehira, K., Hayakawa, T., and Ishikawa, T., *Bull. Chem. Soc. Japan* **51**, 1685 (1978).
8. Takehira, K., Hayakawa, T., and Ishikawa, T., *Bull. Chem. Soc. Japan* **52**, 697 (1979).
9. Takehira, K., Hayakawa, T., and Ishikawa, T., *Bull. Chem. Soc. Japan* **53**, 2103 (1980).
10. Agarwal, A. K., and Srivastava, R. D., *J. Catal.* **45**, 86 (1976).
11. Krishna, L. V. G., Rao, M. S., and Srivastava, R. D., *J. Catal.* **49**, 109 (1977).
12. Prasad, K. M., Athappan, R., and Srivastava, R. D., *J. Catal.* **59**, 460 (1979).
13. Cimino, A., and De Angelis, B. A., *J. Catal.* **36**, 11 (1975).
14. Okamoto, Y., Fujii, M., Imanaka, T., and Teranishi, S., *Bull. Chem. Soc. Japan* **49**, 859 (1976).
15. Nishimura, T., Hayakawa, T., Araki, M., Takehira, K., and Ishikawa, T., *Bull. Japan Petrol. Inst.* **13**, 237 (1971).
16. Clark, G. M., and Doyle, W. F., *Spectrochim. Acta* **22**, 1441 (1966).
17. Gorokhovatskii, Ya. B., *Proc. 5th Int. Congr. Catal., Palm Beach* **1972**, Paper 60.
18. Van Sickle, D. E., Mayo, F. R., and Arluck, R. M., *J. Amer. Chem. Soc.* **87**, 4824 (1965).
19. Prévost-Gagneux, M., Clément, G., and Balaçeanu, J.-C., *Bull. soc. chim. Fr.* **1966**, 2085.
20. Gadelle, C., and Clément, G., *Bull. soc. chim. Fr.* **1967**, 1175.
21. Bateman, L., and Gee, G. *Trans. Faraday Soc.* **47**, 155 (1951).
22. Howard, J. A., and Cobb, J. C., *Trans. Faraday Soc.* **59**, 1590 (1963).
23. Mayo, F. R., and Miller, A. A., *J. Amer. Chem. Soc.* **80**, 2480 (1958).
24. Kamiya, Y., *Kogyo Kagaku Zasshi* **69**, 897 (1966).
25. Ravens, D. A. S. *Trans. Faraday Soc.* **55**, 1768 (1959).
26. Kamiya, Y., and Ingold, K. U., *Canad. J. Chem.* **42**, 1027 (1964).
27. Kamiya, Y., *J. Catal.* **24**, 69 (1972).
28. Scheng, M. N., and Zajacek, J. G., "Oxidation of Organic Compounds," Vol. 2, p. 418. Am. Chem. Soc., 1968.
29. Mukherjee, A., and Graydon, W. F., *J. Phys. Chem.* **71**, 4232 (1967).
30. Fukuzumi, S., Ono, Y., and Keii, T., *Shokubai* **20**, 44p (1978).
31. Kamiya, Y., *Kogyo Kagaku Zasshi* **72**, 8 (1969).
32. Kamiya, Y., Beaton, S., Lafortune, F., and Ingold, K. U., *Canad. J. Chem.* **41**, 2034 (1963).
33. Kamiya, Y., and Ingold, K. U., *Canad. J. Chem.* **42**, 2424 (1964).
34. De Klein, W. J., and Kooyman, E. C., *J. Catal.* **4**, 626 (1965).
35. Mizukami, F., and Imamura, J., *Bull. Chem. Soc. Japan* **51**, 1404 (1978).